



UNIVERSIDADE D
COIMBRA

FACULDADE
DE CIÊNCIAS
E TECNOLOGIA

STUDY ON THE INFLUENCE OF THE STRAIN RATE SENSITIVITY ON THE SPRINGBACK OF THE AA5086 ALLOY UNDER WARM FORMING CONDITIONS

D.M. Neto¹ • M.C. Oliveira¹ • J.L. Alves³ • L.F. Menezes¹

¹ CEMMPRE, Department of Mechanical Engineering, University of Coimbra, Portugal

² CMEMS, Department of Mechanical Engineering, University of Minho, Portugal

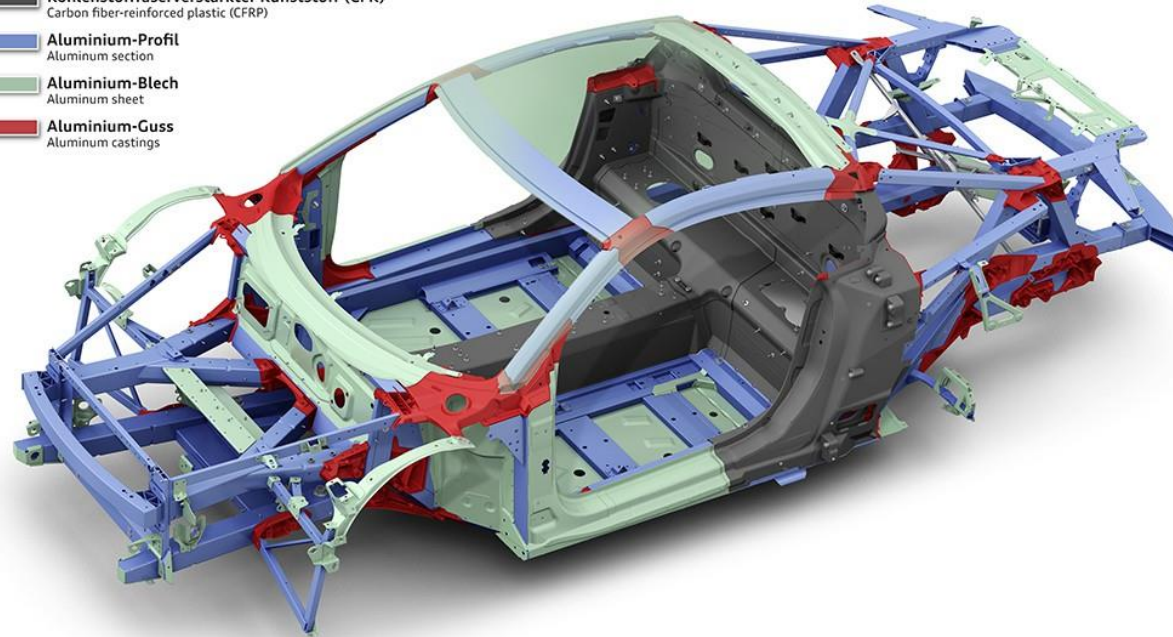
Aluminum alloys

- Increasing use in the **automotive industry** over the past 20 years
- Improve **strength** and reduce **weight** of automotive bodies for **safety** and **fuel efficiency**

Audi R8 Coupé

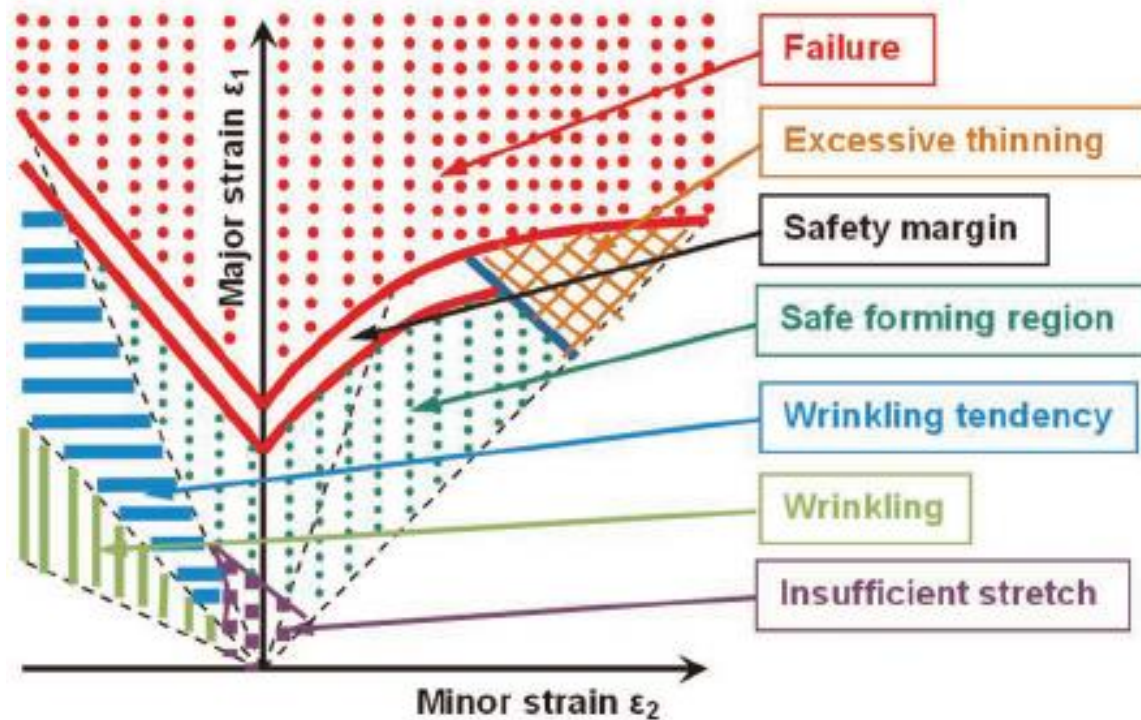
Audi Space Frame in Multimaterialbauweise
Audi space frame in multimaterial construction
03/15

- Kohlenstofffaserverstärkter Kunststoff (CFK)
Carbon fiber-reinforced plastic (CFRP)
- Aluminium-Profil
Aluminum section
- Aluminium-Blech
Aluminum sheet
- Aluminium-Guss
Aluminum castings



Aluminum alloys

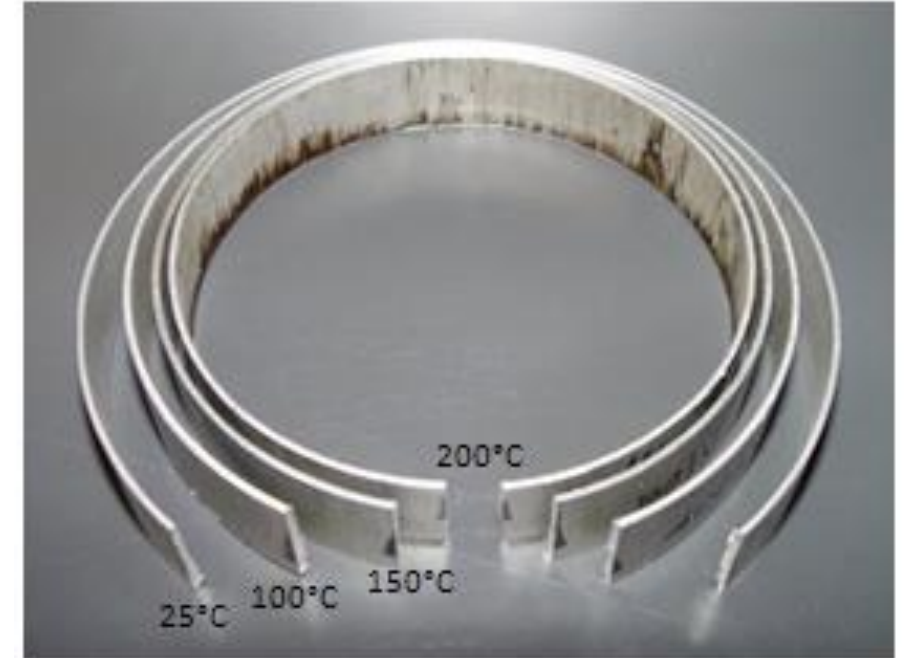
- The main drawbacks of the aluminum alloys are
 - **Poor formability**, particularly at room temperature
 - High values of **springback**, particularly at room temperature



a: Aluminum alloy in cold forming
b: Aluminum alloy in warm forming at 250°C
c: Steel in cold forming

Warm forming of aluminum alloys

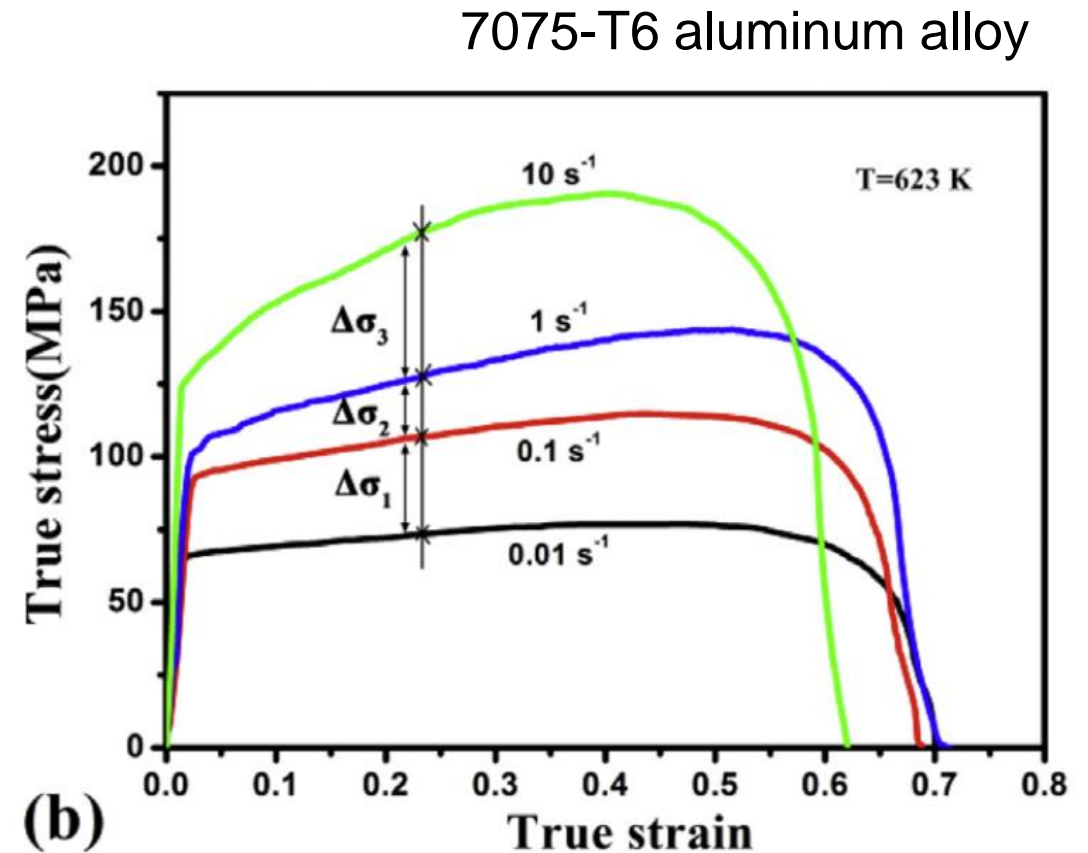
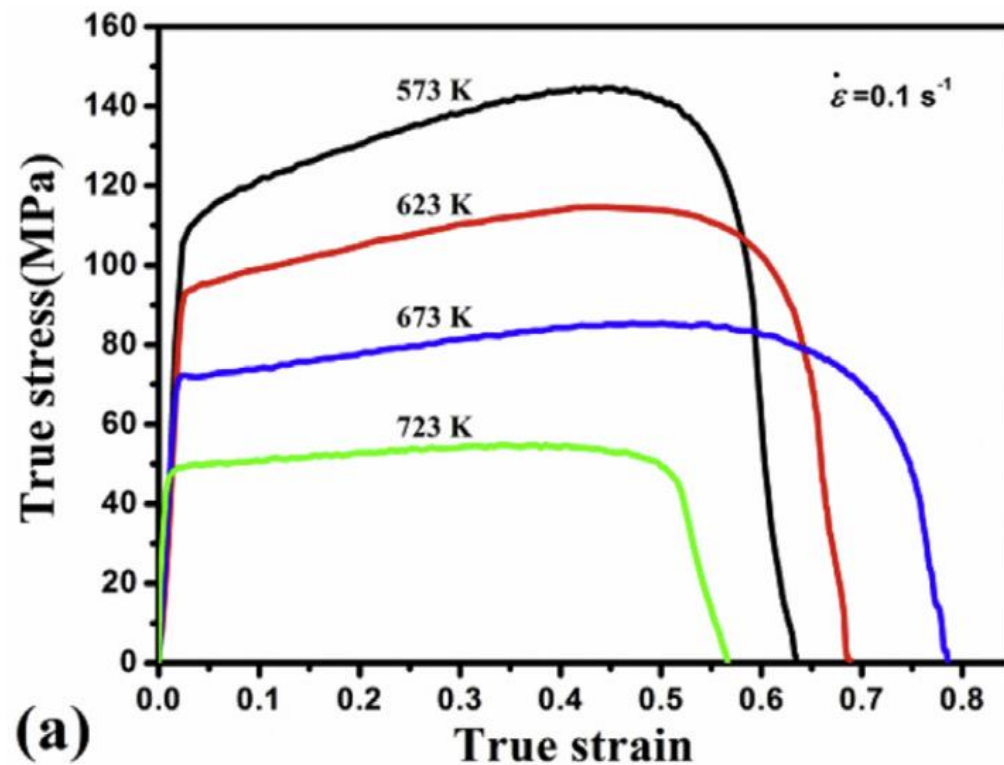
- ❑ Performing the deep drawing operation at an intermediate temperature, leads to a **decrease of the flow stress** and an **increase of ductility**
 - The material **formability** can be improved
 - The **springback** can be reduced
- **Temperature gradient from the bottom to the flange** (heated die and cooled punch) improves formability



Mechanical behavior of aluminum alloys

□ The **stress–strain curves** of the aluminum alloys are influenced by

- Temperature
- Strain rate



Main objective of the study

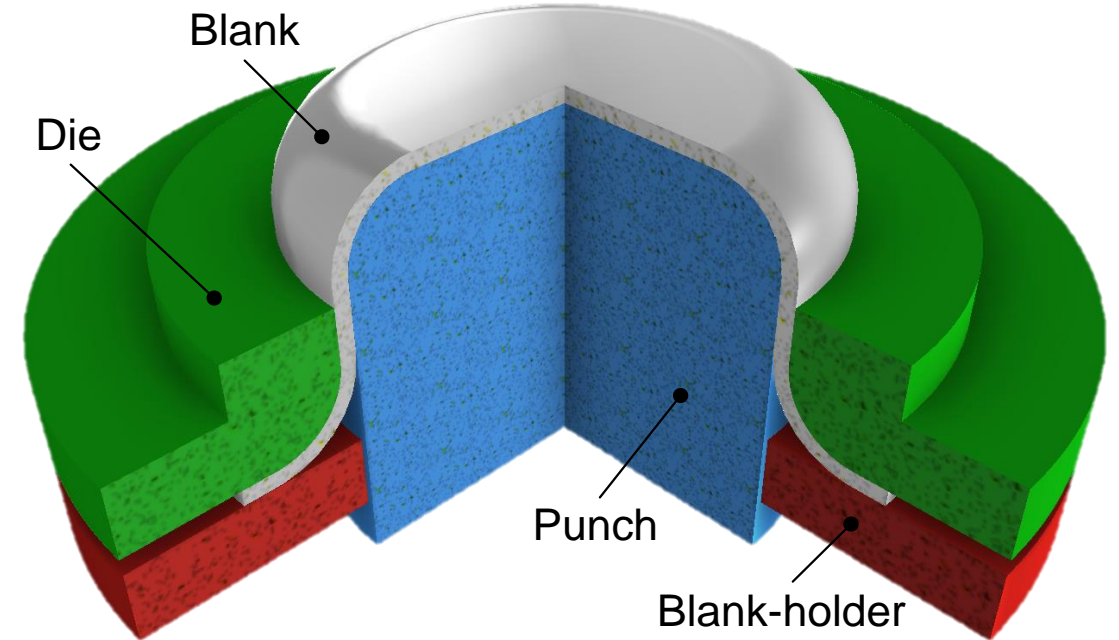
- Analyze the influence of the material **strain rate** sensitivity on the **springback of the split-ring**

Procedure

- **Finite element simulation** of the warm forming process (cylindrical cup) using the non-isothermal conditions defined in Benchmark 3 of the Numisheet 2016 conference
- The blank is from an **AA5086 aluminum alloy**
- The mechanical behavior is described by a **rate-dependent thermo-elasto-plastic** law
- The parameters of the hardening law are calibrated using data from **uniaxial tensile tests at different temperatures and strain rate values**

Deep drawing of an aluminum cylindrical cup at warm temperature

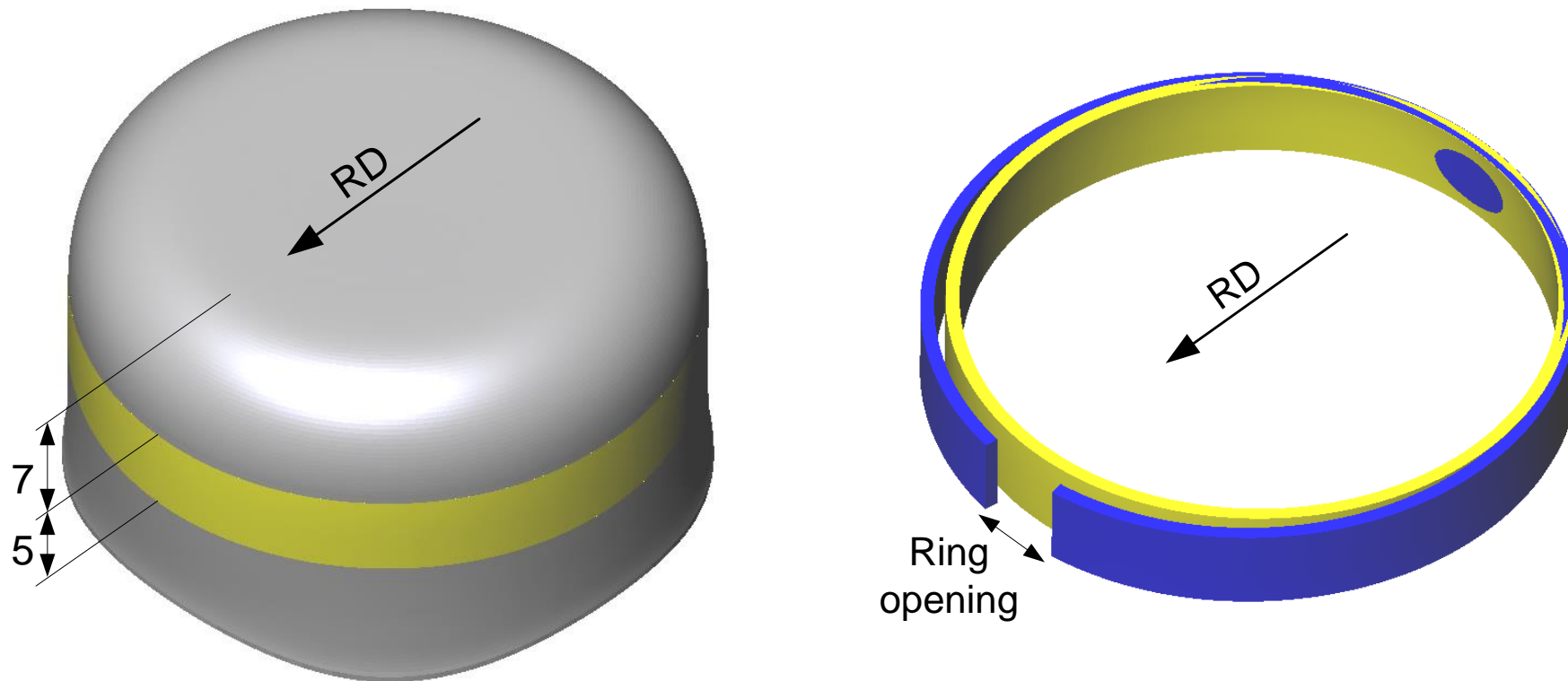
- The punch diameter is 33 mm. Both the punch and the die present a corner radius of 5 mm
- The **blank is circular** (60 mm of diameter) with 0.8 mm of nominal thickness
- Blank-holder force (5 kN) constant until the cup is fully drawn



- Different values of **constant punch speed**
 - 0.05 mm/s
 - 0.5 mm/s
 - 5 mm/s
- } Distinct values of the strain rate

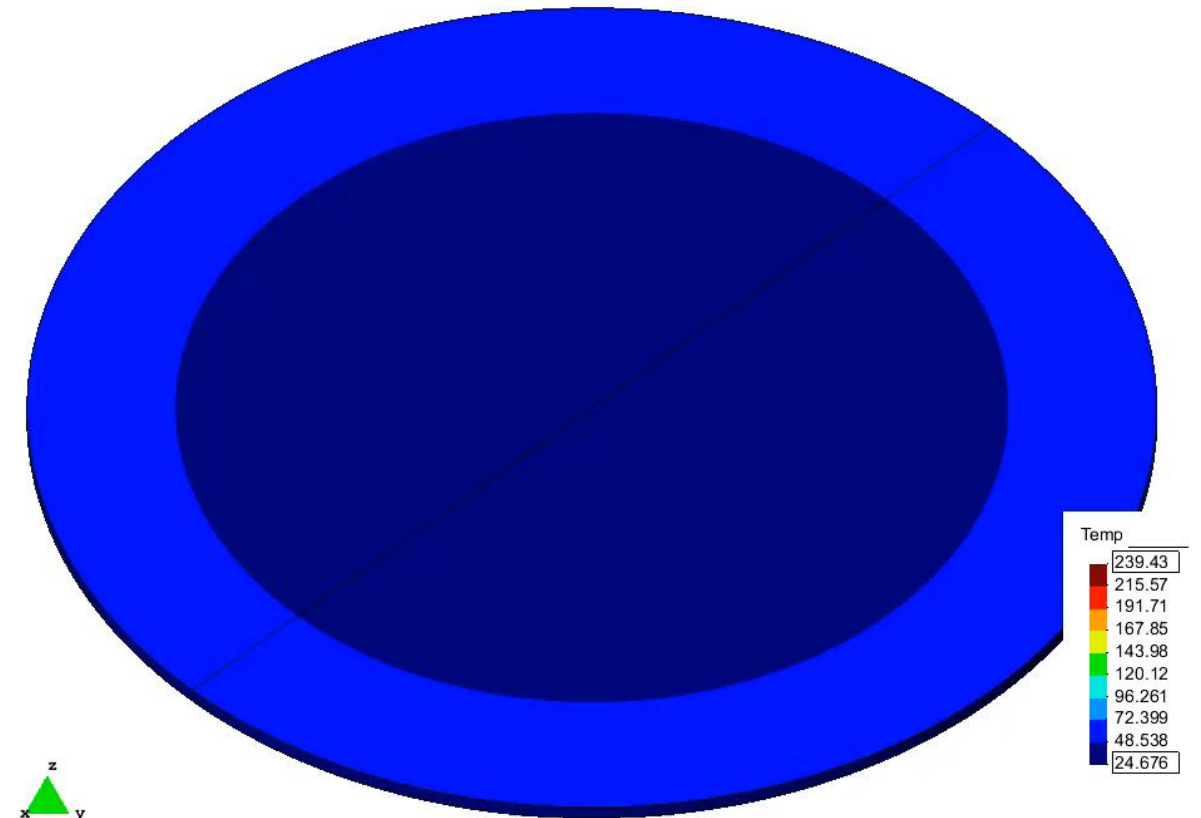
Deep drawing of an aluminum cylindrical cup at warm temperature

- Both the **die and the blank-holder are heated** (240°C), while the punch is water cooled
- **Springback** resulting from the residual stresses is evaluated through the **split-ring test** (Demeri test) by measuring the **opening of a ring** cut from the sidewall of the cylindrical cup



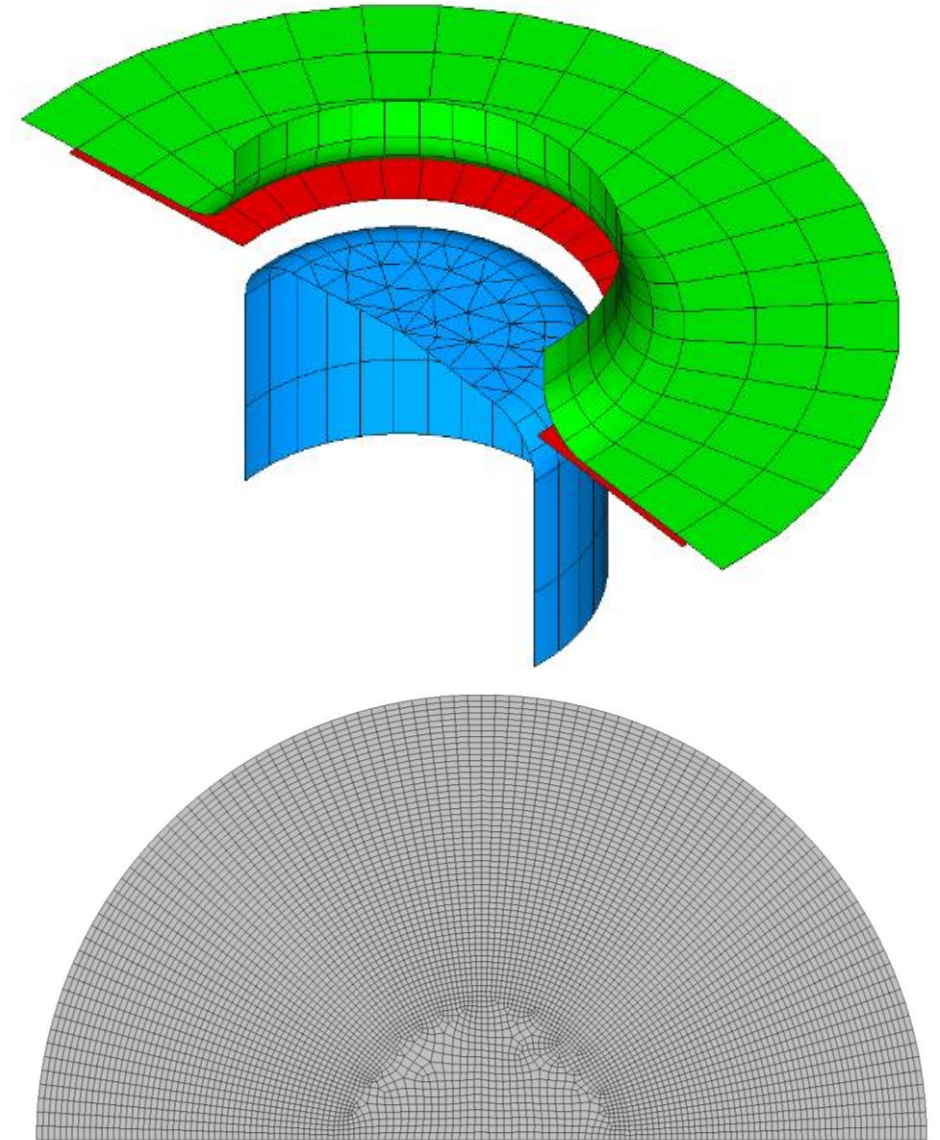
Numerical model

- ❑ Numerical analysis carried out using the **DD3IMP** in-house finite element code
- ❑ Numerical simulation divided into **6 stages**
 1. Heating of the blank within the tools
 2. Deep drawing operation
 3. Cooling of the cup
 4. Unloading the cup
 5. Cutting the ring
 6. Split the ring



Numerical model

- **Half geometry** is simulated (symmetry conditions)
- **Forming tools** are assumed **rigid and isothermal** (described by Nagata patches)
 - Die and the blank-holder at 240°C
 - Punch at 70°C
- Blank is discretized using **11,970 linear hexahedral finite elements**
- Friction modelled by the **Coulomb's law** ($\mu=0.09$)
- **Interfacial heat transfer coefficient** is 2500 W/(m²K)



Material modelling

- **Rate-dependent thermo-elasto-plastic** material constitutive model
- Elastic behavior described by the **Hooke's law** (isotropic and temperature-independent)

Young modulus [GPa]	Poisson's ratio
71.7	0.31

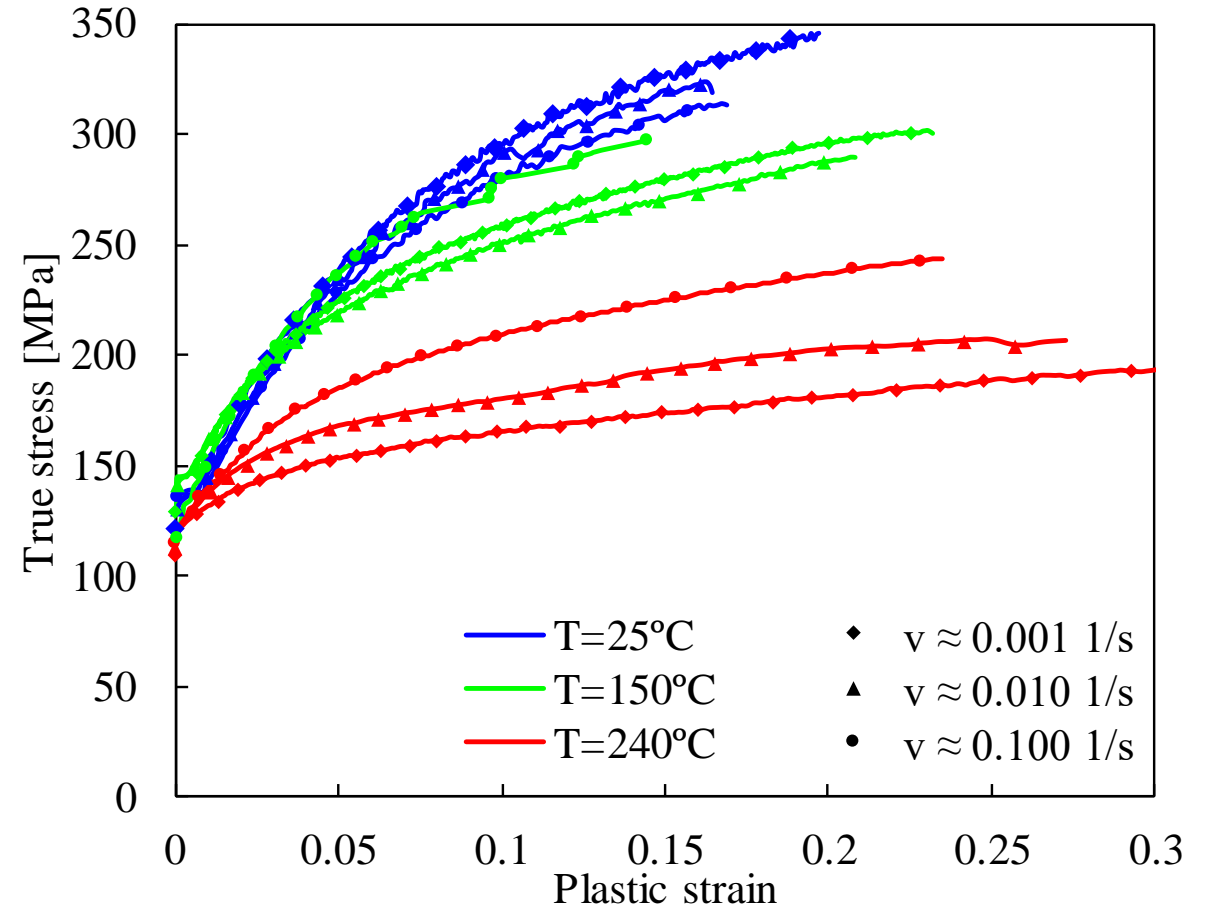
- **Thermal properties** of the AA5086 aluminum alloy used in the numerical model

Mass density [kg/m ³]	Specific heat [J/kg ⁰ C]	Conductivity [W/m ⁰ C]
2700	900	220

Material modelling

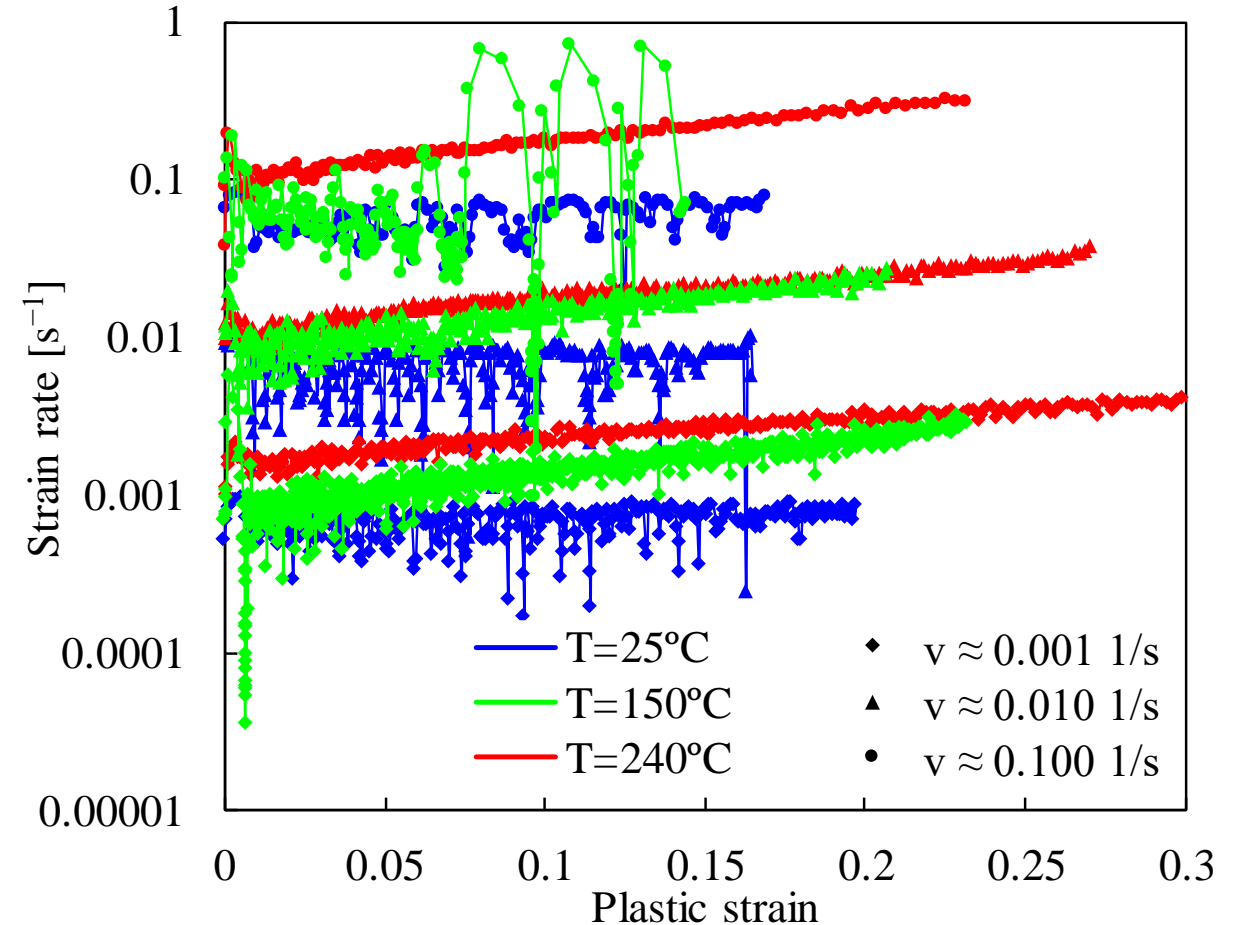
□ **Stress–strain curves (experimental)** from uniaxial tensile tests carried out at different temperatures and distinct values of crosshead velocity

- Increasing the test temperature leads to a decrease of the flow stress
- The strain rate sensitivity is more visible at warm temperatures
- Negative strain rate sensitivity at room temperature
- Positive strain rate sensitivity at 240°C



Material modelling

- Evolution of the **strain rate** in each uniaxial tensile tests
 - Slightly increase of the strain rate during the test, particularly for warm temperatures
 - 3 distinct levels for the strain rate can be identified
 - $v \approx 0.001 \text{ s}^{-1}$
 - $v \approx 0.01 \text{ s}^{-1}$
 - $v \approx 0.1 \text{ s}^{-1}$



Material modelling

□ Hockett–Sherby hardening law

- Flow stress at different values of temperature and strain rate

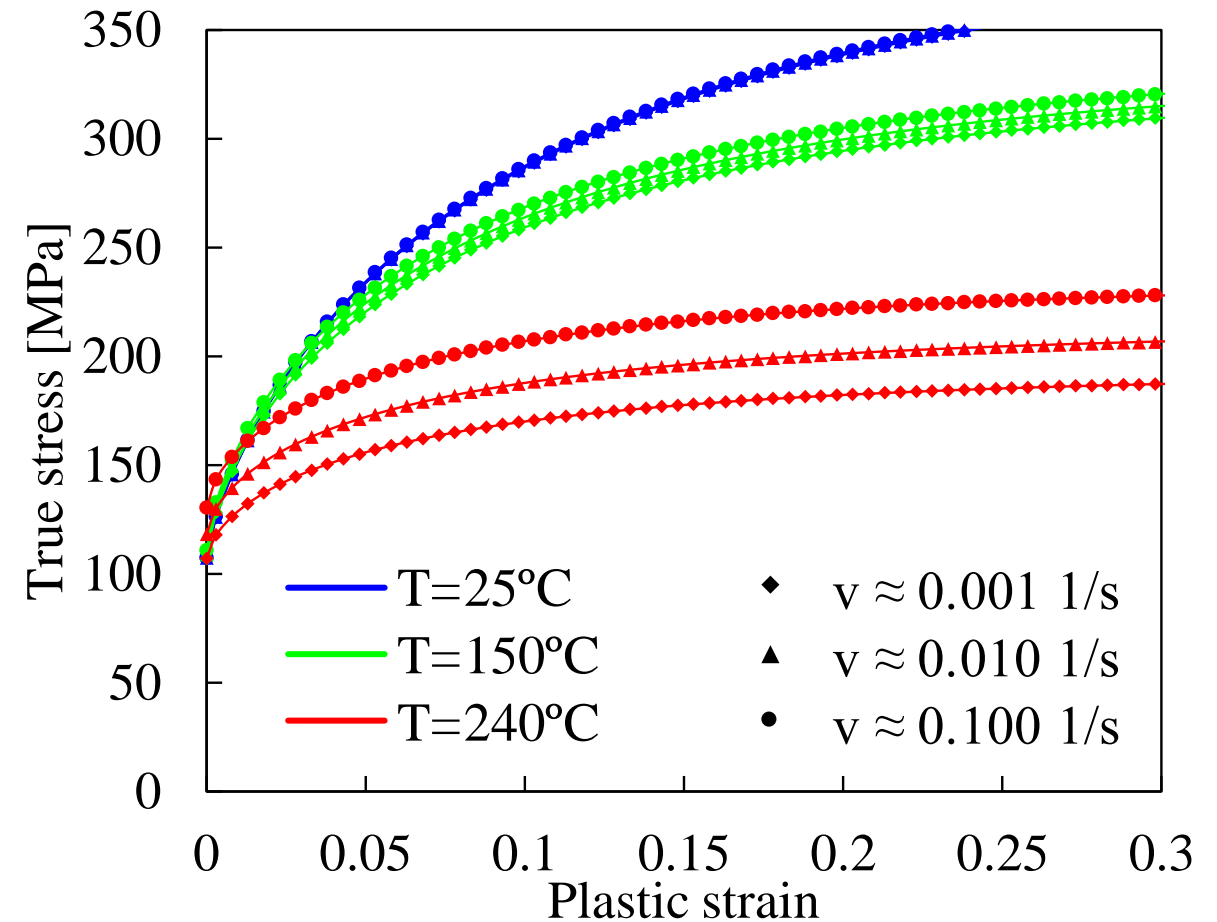
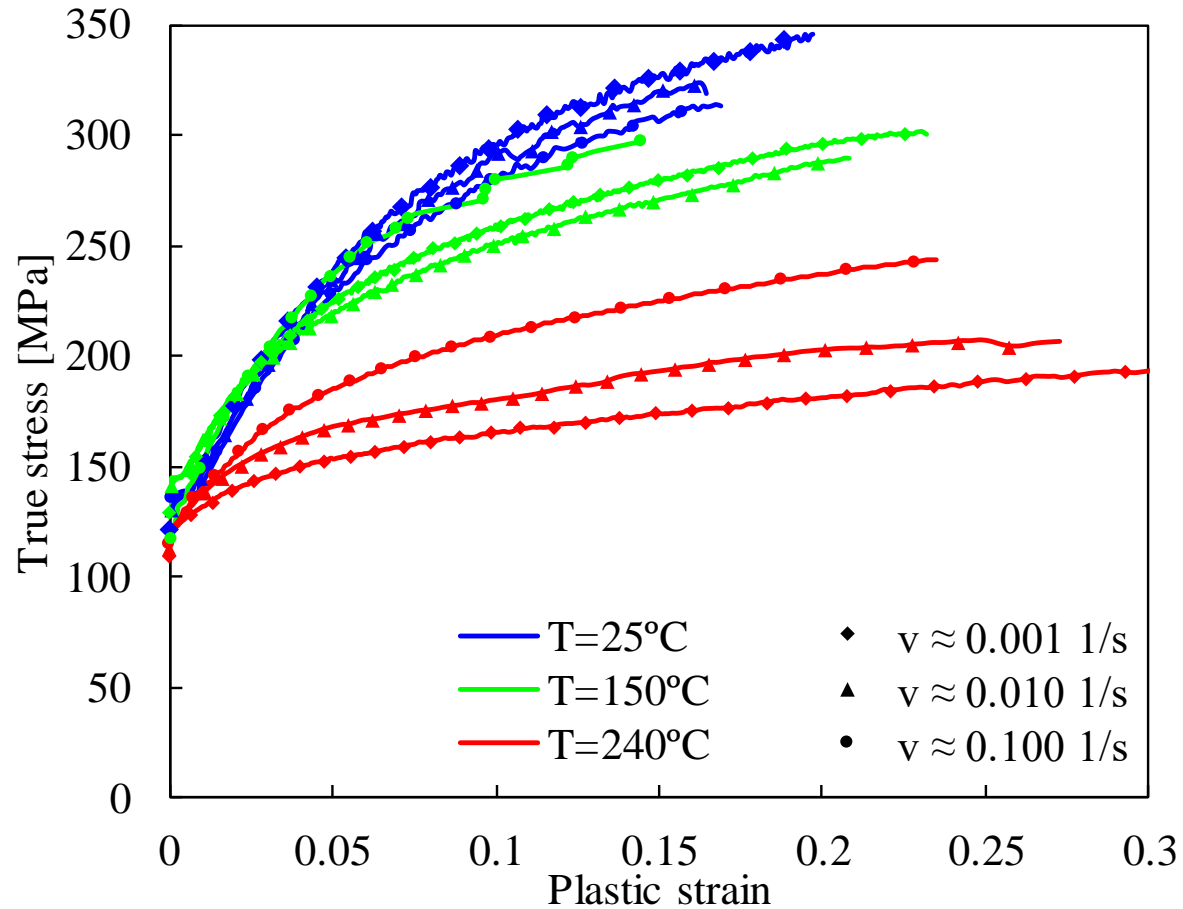
$$Y = \left\{ Y_0 + \left(Q_0 + a_1 \left(1 - \exp \left(a_2 \frac{T}{T_m} \right) \right) \right) \left(1 - \exp \left(-b (\bar{\varepsilon}^p)^{\left\{ n_0 - n_1 \left(\frac{T}{T_m} \right) \right\}} \right) \right) \right\} \left(\frac{\dot{\varepsilon}}{\dot{\varepsilon}_0} \right)^{\left\{ m_0 \exp \left(m_1 \frac{T}{T_m} \right) \right\}}$$

- The parameters were obtained through the minimization of the difference between the numerical and the experimental stress values

Y_0 [MPa]	Q_0 [MPa]	a_1 [MPa]	a_2	b	n_0	n_1	m_0	m_1	ε_0 [s ⁻¹]	T_m [°C]
107.07	286.81	17.43	6.32	5.92	0.78	0.32	4.2×10^{-4}	11.58	0.001	600

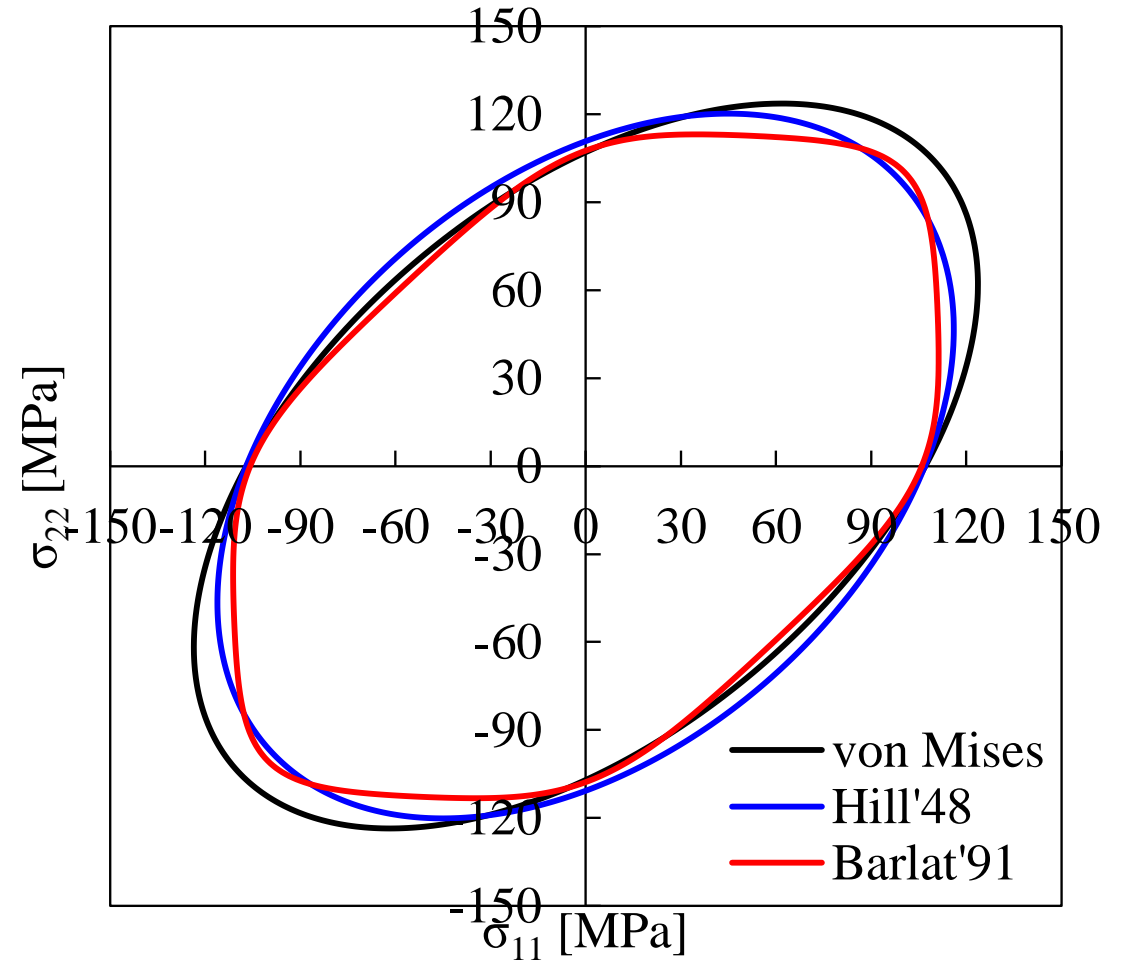
Material modelling

- Comparison between **experimental** and **numerical** stress–strain curves



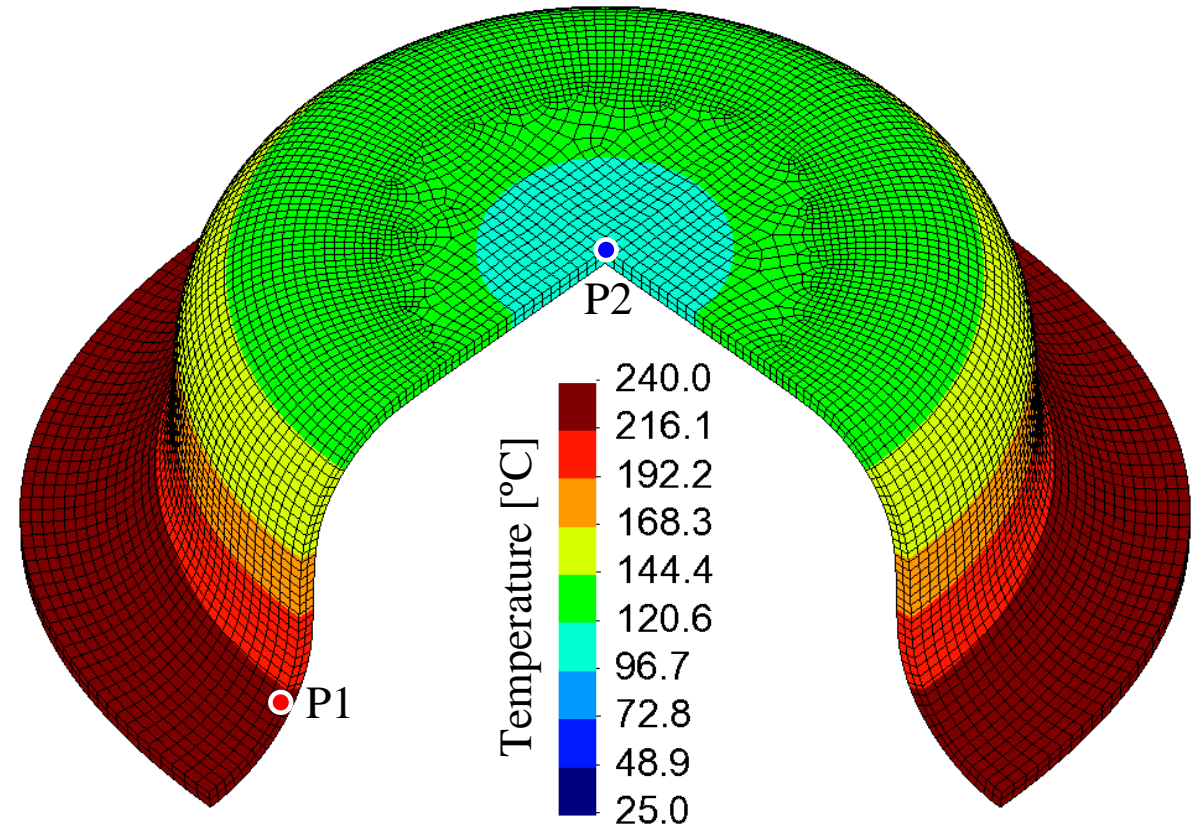
Material modelling

- ❑ Plastic anisotropy (temperature-independent) modelled using two different yield criteria (**Hill'48** and **Barlat'91**)
- Parameters of the Hill'48 yield criterion evaluated based on the anisotropy coefficients (r -values) measured at 240°C
- The parameters of the Barlat'91 yield criterion evaluated using both the yield stresses and the anisotropy coefficients, measured at 240°C



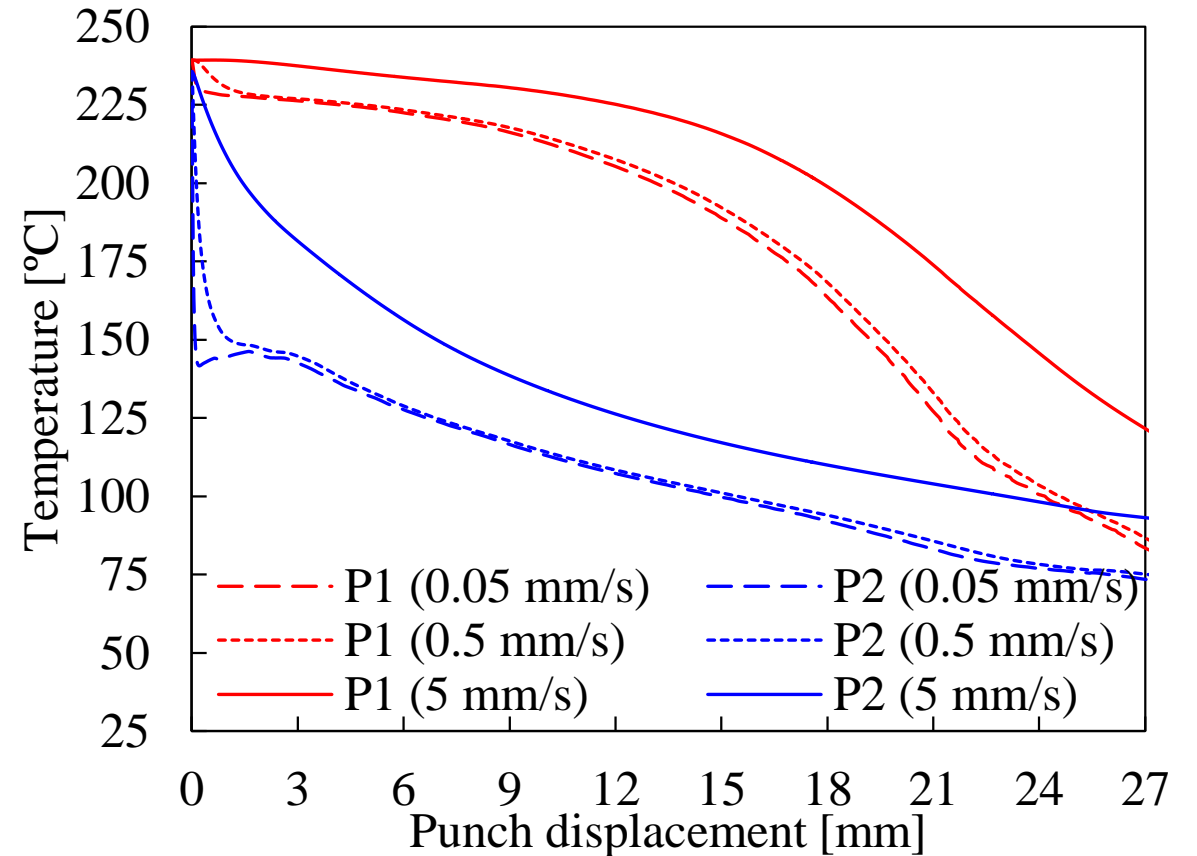
Temperature distribution

- **Predicted temperature distribution** in the cylindrical cup for a punch displacement of 15 mm (**5 mm/s of punch velocity** and the Hill'48 yield criterion)
- The temperature distribution is roughly axisymmetric
- Minimum value in the bottom center (P2) and the maximum value in the flange



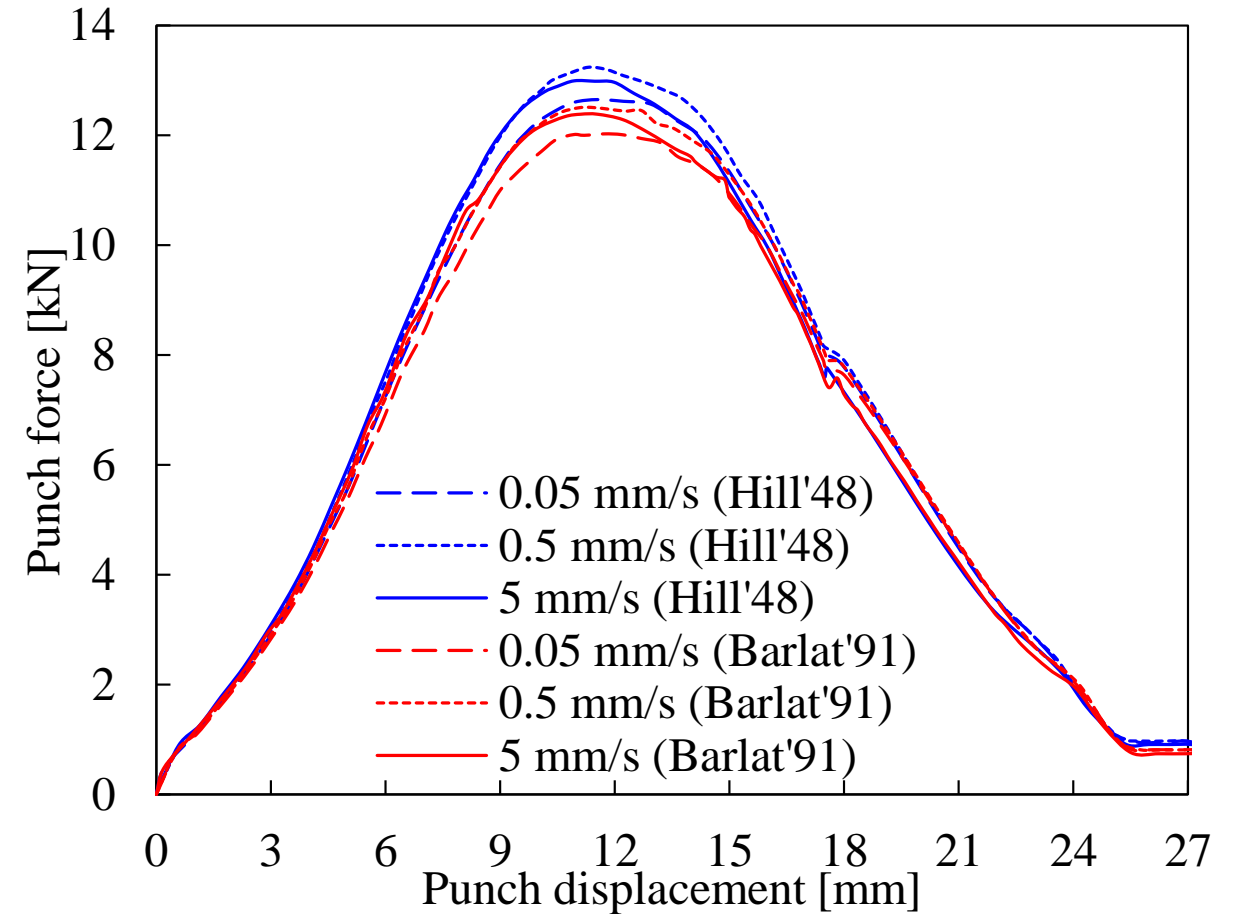
Temperature distribution

- **Influence of the punch velocity** on the predicted temperature distribution.
Temperature evaluated in 2 points (P1 and P)
- The **decrease of the punch velocity** yields to a global **decrease of the cup temperature** (increase of the time to promote heat losses with the cold punch)



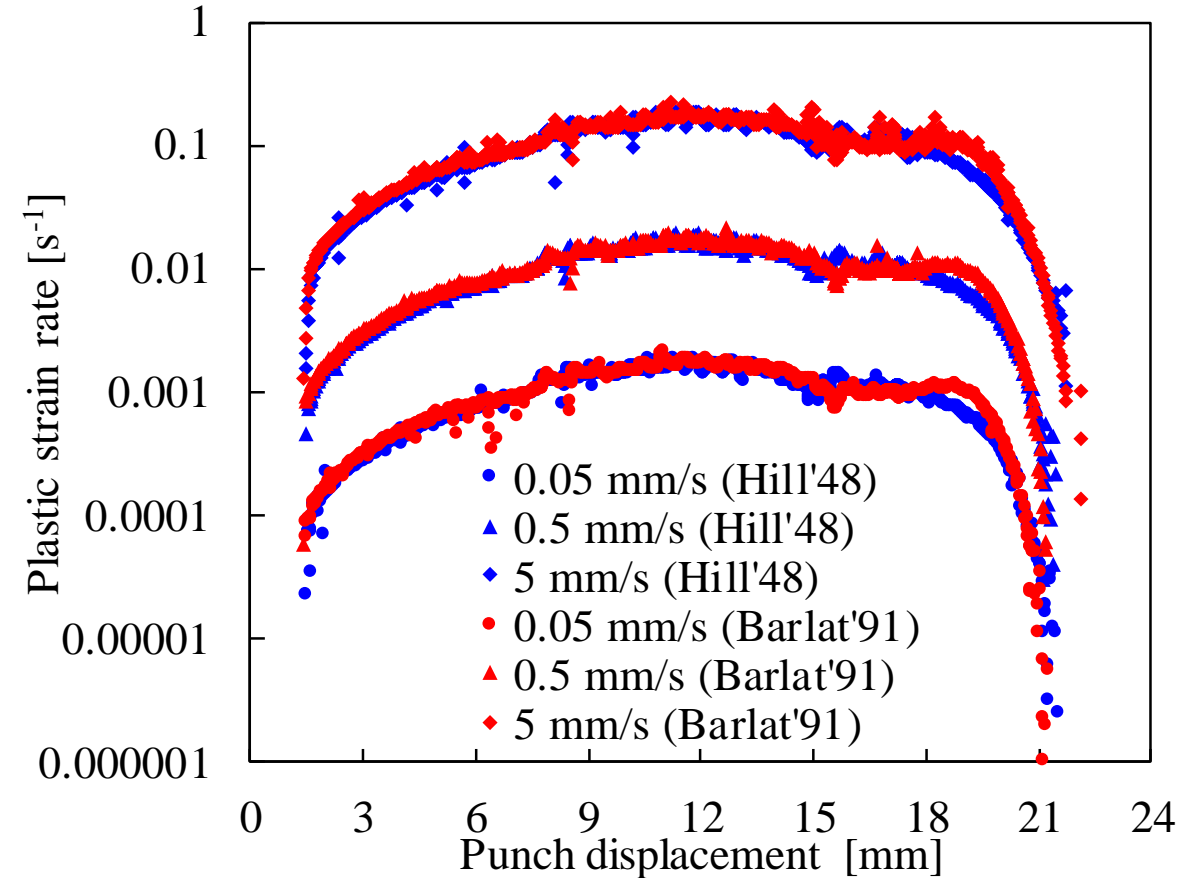
Punch force

- Predicted **punch force evolution** for different values of punch velocity
- Influenced by the **temperature distribution** and the **strain rate in the cup**
- The punch force evolution presents an **increase when the punch velocity increases** from 0.05 mm/s to 0.5 mm/s due to the positive strain rate sensitivity



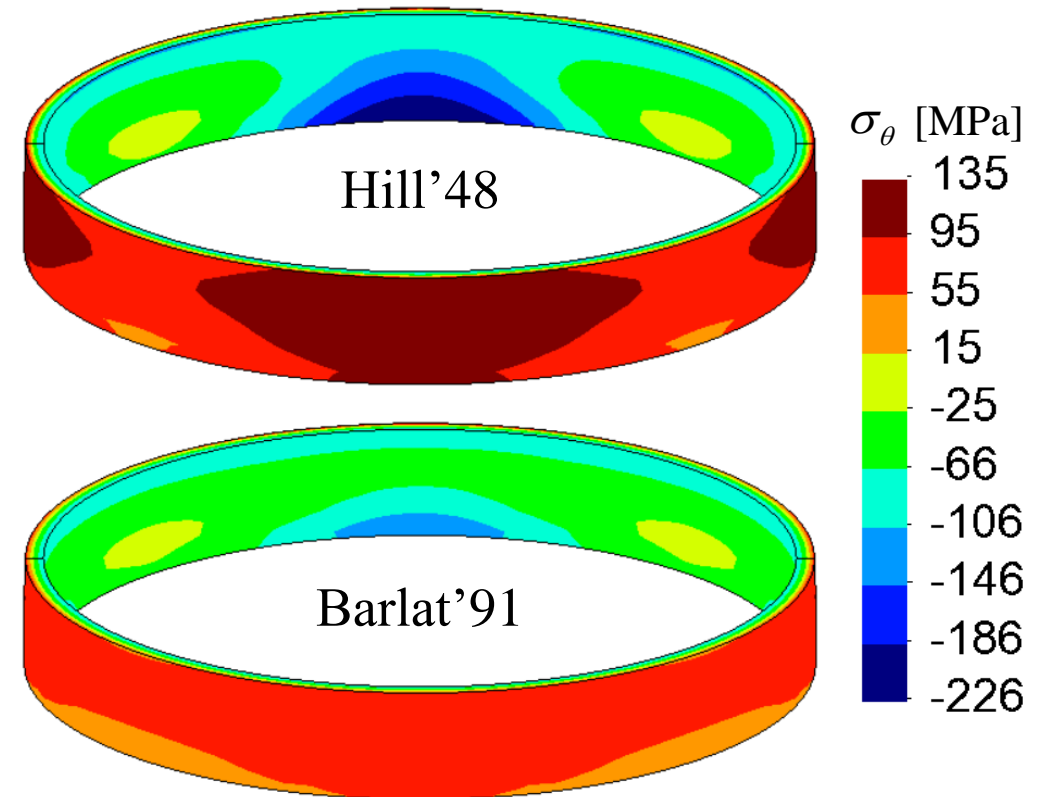
Plastic strain rate

- Evolution of the **plastic strain rate** evaluated in a point initially located in the flange (5 mm from the free edge), comparing 3 different values of punch velocity
- The relationship between the punch velocity and the predicted plastic strain rate is **approximately linear**
- For 5 mm/s of punch velocity, the plastic strain rate ranges from about 0.01 s^{-1} up to 0.1 s^{-1}



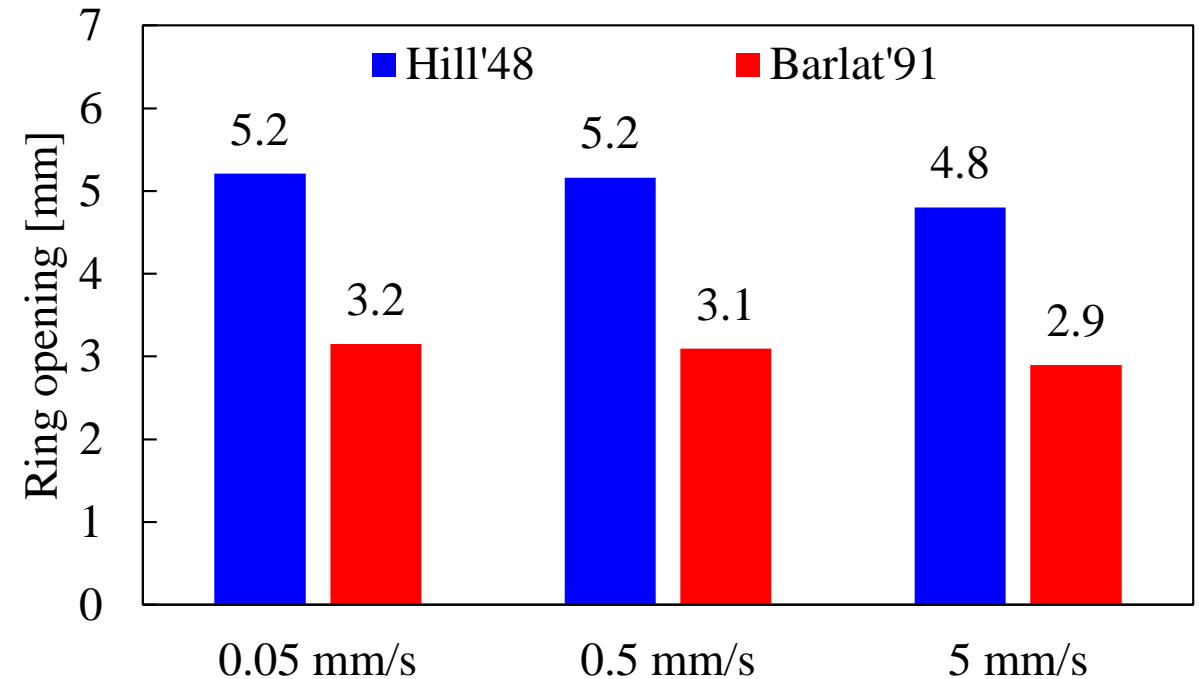
Split-ring test

- Numerical analysis of the **split-ring test** after cooling down to **room temperature**
- Predicted distribution of the **hoop stress on the ring** (before splitting) for 0.05 mm/s of punch velocity
 - Compressive in the inner surface of the ring and tensile on the outer surface
 - Slight variation along the circumferential direction due to the plastic anisotropy



Split-ring test

- Predicted values of **ring opening** for 3 different values of punch velocity
- The **impact of the punch velocity** on the springback value is **negligible** since it is always evaluated at room temperature
- **Lower ring opening** predicted by the **Barlat'91** yield criterion due to the lower hoop stress gradient through the thickness



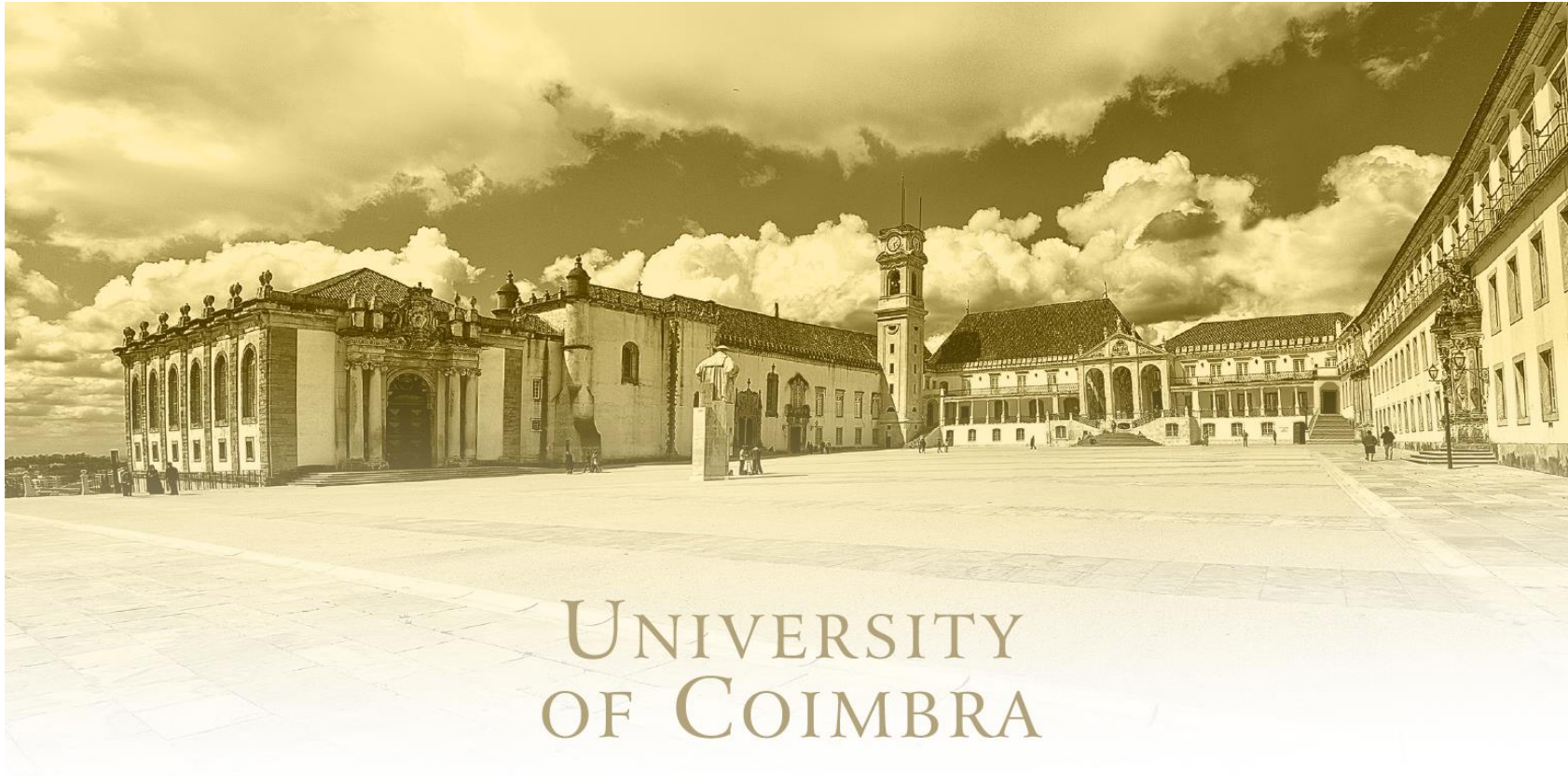
- **Warm forming simulation** of a cylindrical cup (AA5086) using heated die/blank-holder and cooled punch
- Study the effect of the **strain rate** (controlled by the punch velocity) on the **springback**, evaluated by means of the split-ring test
- Numerical analysis using a **rate-dependent thermo-elasto-plastic** hardening law
- Calibration of the parameters of the Hockett–Sherby hardening law using experimental data from uniaxial tensile tests performed at different temperatures and strain rates
- The predicted **springback is strongly influenced by the yield function** adopted to model the material anisotropy
- **The impact of the punch velocity (i.e. strain rate) on the springback is negligible** since the hoop stress distribution on the ring (before splitting) is only slightly influenced by the punch velocity

This work was funded by the Portuguese Foundation for Science and Technology (FCT) under projects with reference PTDC/EME-EME/30592/2017 and PTDC/EME-EME/31657/2017 and by European Regional Development Fund through the Portugal 2020 program and the Centro 2020 Regional Operational Programme (CENTRO-01-0145-FEDER-031657) under the project MATIS (CENTRO-01-0145-FEDER-000014) and UIDB/00285/202020.

Projetos Cofinanciados pela UE:



UNIÃO EUROPEIA
Fundo Europeu
de Desenvolvimento Regional



Thank you for watching!